Journal of the Brazilian Society of Mechanical Sciences and Engineering (2018) 40:76
https://doi.org/10.1007/s40430-018-1019-6

TECHNICAL PAPER

Approximate analytical methodology for calculating friction factors in flow through polygonal cross section ducts

M. C. Reis[1] · L. A. Sphaier[1] · L. S. de B. Alves[1] · R. M. Cotta[2]

Received: 6 February 2017 / Accepted: 18 September 2017 / Published online: 24 January 2018

Abstract
An approximate analytical methodology for calculating the friction factor within ducts of irregular cross-section is herein proposed. The approximations are developed by transforming the original governing PDEs into simpler ODEs, using approximation rules provided by the coupled integral equations approach. The transformed system is directly integrated and analytical solutions for the friction factor are readily obtained. Four different approximation cases are analyzed, which yield simple closed-form expressions for calculating the friction factor in terms of geometric parameters for rectangular, triangular, and trapezoidal ducts. The results of these expressions are compared with literature data, and very reasonable agreement is seen. After performing an error analysis of the results, regions for applicability of the methodology where accuracy requirements can be maintained are highlighted. Finally, enhanced approximation formulas yielding maximum errors as low as 3% are developed by using simple weighted averages of different approximation cases.

Keywords Lumped-capacitance formulation · Arbitrary geometry · Friction factor · Mathematical modeling

List of symbols

a, b, c	Geometric parameters in cross-section domain
D_H	Hydraulic diameter
f	Fanning's friction-factor
G^*	Dimensionless pressure gradient
$H_{\alpha,\beta}$	Hermite approximation
K	Aspect ratio
p	Pressure
u	Axial velocity
$\bar{u}$	Cross-sectional averaged velocity
U	Dimensionless axial velocity
x	Axial variable
X	Dimensionless function for left boundary
y, z	Cross-section variables
Y, Z	Dimensionless problem variables
z_1	Function for left boundary
Re	Reynolds number

Greek symbols

α, β, ν	Hermite approximation parameters
ξ, η	Dimensionless left boundary function parameters
μ	Dynamic viscosity
ζ_i	Solution constants

1 Introduction

Scientists working on applied mathematics found themselves in the perfect environment to develop numerical methods with the introduction of computers and the fast increase of their memory capacity and processing speed over the subsequent decades. These methods became so reliable that, nowadays, they are routinely utilized in commercial packages devoted to the simulation of engineering problems. However, they are widespread to the point of discouraging the use of analytical methods, often being applied to solve problems that do posses analytical solutions. Analytical methodologies played a crucial role in the early development of fluid mechanics and heat transfer and their relevance should not be overlook even today.

One important example in the field of differential equations is the combined use of analytical and numerical

Technical Editor: Jader Barbosa Jr.

✉ L. A. Sphaier
lasphaier@id.uff.br

[1] Department of Mechanical Engineering – TEM/PGMEC, Universidade Federal Fluminense – UFF, Rua Passo da Pátria 156, sala 302, bloco D, Niterói, RJ 24210-240, Brazil

[2] Laboratório de Transmissão e Tecnologia do Calor – LTTC, Departamento de Engenharia Mecânica – POLI/COPPE, Universidade Federal do Rio de Janeiro, Rio de Janeiro, RJ 21945-970, Brazil

methods to generate lumped solutions. These solutions are obtained from an approximately averaged version of the differential equations, created using special analytical techniques that reduce their number of spatial dimensions. However, it is important to control the error introduced by such approximations in order to maintain precision requirements. One particular technique that achieves these goals is known as coupled integral equations approach or CIEA. It approximates an integral by a linear combination of the integrand and its derivatives at the integration limits, an idea originally developed by Hermite [1] and first presented by Mennig et al. [2]. The latter were the first ones to use this two-point approach, deriving it in a fully differential form called $H_{\alpha,\beta}$. Furthermore, these authors showed that the already known Obreschkoff formulae presented no new features in relation to the $H_{\alpha,\beta}$ method. They used this technique to solve linear initial-value and boundary-value ODEs, demonstrating the advantages of this approach compared to other methods.

Since its development, the CIEA has been applied to many problems. Among these studies, deserve mention the ones involving phase change [3], heat transfer in fins [4], heat exchangers [5, 6], linear heat conduction [7], hyperbolic heat conduction [8], radiative cooling [9], ablation [10], drying [11], heat diffusion with temperature-dependent conductivity [12], and combined convective-radiative cooling [13, 14]. A very similar approach was also used in the work of Keshavarz and Taheri [15]. However, the authors refer to it by a different name, calling it the Polynomial Approximation Method. Another similar approach for obtaining improved lumped-models was employed by Sadat [16, 17], in which general transient diffusion problems were considered. In more recent years, the CIEA methodology was applied for the solution of coupled heat and mass transfer in adsorbed gas reservoirs [18], heat conduction in phase change materials [19], thermal modeling of building elements [20] and multilayered composite pipelines with active heating [21].

The current paper presents an approximate analytical methodology, based on the coupled integral equations approach, for solving steady laminar fluid flow equation in irregular geometries. Its ultimate goal is to obtain simple expressions for the friction factor for these flows, and to analyze the error associated with each of these. Results for different polygonal cross-section ducts, which include rectangular, trapezoidal, and triangular geometries, are obtained using four different approximation cases. A comprehensive comparison of the different approximation cases is carried-out, demonstrating that some approximation schemes could lead to errors that are too large for certain geometric parameters. As a result of this analysis, further enhanced approximate expressions for calculating the friction factor in rectangular, triangular and trapezoidal duct geometries are proposed.

2 Hermite approximation

The basis for the coupled integral equations approach (CIEA) is the Hermite approximation of an integral, which is given by the general expression:

$$\int_{x_{i-1}}^{x_i} f(x)\mathrm{d}x = \sum_{v=0}^{\alpha} c_v(\alpha,\beta) h_i^{v+1} f^{(v)}(x_{i-1}) + \sum_{v=0}^{\beta} c_v(\beta,\alpha)(-1)^v h_i^{v+1} f^{(v)}(x_i) + E_{\alpha,\beta} \tag{1a}$$

where,

$$h_i = x_i - x_{i-1}, \quad c_v(\alpha,\beta) = \frac{(\alpha+1)!(\alpha+\beta-v+1)!}{(v+1)!(\alpha-v)!(\alpha+\beta+2)!} \tag{1b}$$

and $f(x)$ and its derivatives $f^{(v)}(x)$ are defined for all $x \in [x_{i-1}, x_i]$. $E_{\alpha,\beta}$ is the error in the approximation. It is assumed that $f^{(v)}(x_{i-1}) = f_{i-1}^{(v)}$ for $v = 0, 1, 2, \ldots, \alpha$ and $f^{(v)}(x_i) = f_i^{(v)}$ for $v = 0, 1, 2, \ldots, \beta$. This integration formula can easily provide different levels of approximation, which are traditionally called $H_{\alpha,\beta}$. Nevertheless, since approximations of order higher than $H_{1,1}$ involve derivatives of order higher than one, these are avoided for the sake of simplicity of the methodology. Hence, only two different approximations below are considered:

$$H_{0,0} \Rightarrow \int_0^h f(x)\mathrm{d}x \approx \frac{1}{2}h(f(0)+f(h)), \tag{2a}$$

$$H_{1,1} \Rightarrow \int_0^h f(x)\mathrm{d}x \approx \frac{1}{2}h(f(0)+f(h)) + \frac{1}{12}h^2(f'(0)-f'(h)), \tag{2b}$$

which correspond to the well known trapezoidal and corrected trapezoidal integration rules, respectively.

3 Laminar flow in polygonal cross-section ducts

In this section, the integral approximation rules (2a, 2b) are applied to fully-developed laminar flow in straight ducts of irregular geometry cross-sections, allowing expressions for the friction-factor for different types of ducts to be obtained. Figure 1 displays the general problem domain

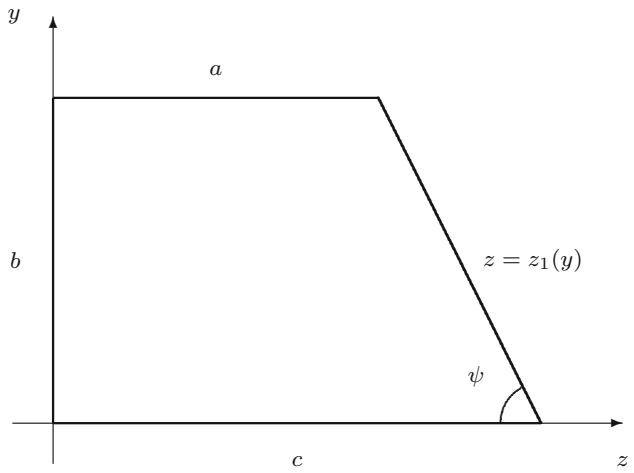

Fig. 1 Problem domain

with the adopted geometric parameters. The function $z_1(y)$ describes the right boundary between $y = a$ and $y = c$.

The governing equations for the considered problem, in dimensionless form, are given by:

$$\frac{\partial^2 U}{\partial Y^2} + K^2 \frac{\partial^2 U}{\partial Z^2} = G^*, \quad \text{for} \quad 0 \le Y \le 1 \quad \text{and} \quad 0 \le Z \le X(Y), \tag{3a}$$

$$U = 0, \quad \text{for} \quad Y = 0 \quad \text{and} \quad 0 \le Z \le 1, \tag{3b}$$

$$U = 0, \quad \text{for} \quad Y = 1 \quad \text{and} \quad 0 \le Z \le 1, \tag{3c}$$

$$\frac{\partial U}{\partial Z} = 0, \quad \text{for} \quad Z = 0 \quad \text{and} \quad 0 \le Y \le 1, \tag{3d}$$

$$U = 0, \quad \text{for} \quad Z = X(Y) \quad \text{and} \quad 0 \le Y \le 1, \tag{3e}$$

in which the involved dimensionless groups are defined as:

$$Y = \frac{y}{b}, \quad Z = \frac{z}{a}, \quad U = \frac{u}{\bar{u}}, \quad K = \frac{b}{a}, \quad G^* = \frac{b^2}{\mu \bar{u}} \frac{\mathrm{d}p}{\mathrm{d}x}, \tag{4}$$

where $X(Y) = \xi Y + \eta$ is the dimensionless form of $z_1(y)$, where ξ and η are geometric parameters:

$$\xi = -K \cot(\psi) \quad \text{and} \quad \eta = 1 + K \cot(\psi). \tag{5}$$

The expression of Fanning's friction-factor can be readily expressed in terms of the dimensionless pressure gradient as:

$$f \,\mathrm{Re} = -\frac{G^*}{2} \frac{D_\mathrm{H}^2}{b^2}, \tag{6}$$

in which G^* is the dimensionless pressure gradient [defined by Eq. (4)], and Re is the hydraulic-diameter based Reynolds number. The hydraulic diameter itself is expressed as:

$$\frac{D_\mathrm{H}}{b} = \frac{4 + 2K \cot(\psi)}{2 + K\left(\csc(\psi) + \cot(\psi)\right)}, \tag{7}$$

where b is a length, as described in Fig. 1. Finally, the horizontal-averaged velocity is defined as:

$$U_{av}(Y) = \frac{\int_0^X U(Y,Z)\,\mathrm{d}Z}{\xi Y + \eta}. \tag{8}$$

With little algebraic manipulation, the integration of Eqs. (3a, 3b, 3c) within $0 \le Z \le X$ and substitution of Eqs. (3d, 3e) and (8), yields:

$$\frac{\mathrm{d}^2 U_{av}}{\mathrm{d}Y^2} + \frac{2\xi}{\xi Y + \eta} \frac{\mathrm{d}U_{av}}{\mathrm{d}Y} + \frac{(K^2 + \xi^2)}{\xi Y + \eta} \left.\frac{\partial U}{\partial Z}\right|_{Z=X} = G^*, \quad \text{for} \quad 0 \le Y \le 1, \tag{9a}$$

$$U_{av} = 0, \quad \text{at} \quad Y = 0 \quad \text{and} \quad Y = 1, \tag{9b}$$

where the following relation between the Y- and Z-derivatives of U at $Z = X$, obtained from the boundary condition at this location (3e), was used for simplification:

$$\left.\frac{\partial U}{\partial Y}\right|_{Z=X} = -\xi \left.\frac{\partial U}{\partial Z}\right|_{Z=X}. \tag{10}$$

Equation (9) constitute an exact form of system (3) that was transformed to eliminate the independent variable Z. In spite of being a simpler system, in order to solve Eq. (9), the derivatives of the two-dimensional velocity field U at $Z = X(Y)$ must be expressed in terms of the Z-averaged velocity, $U_{av}(Y)$. However, no further exact transformations can be of assistance at this point, and approximation rules must be employed.

By inspecting Eqs. (9a) and (10), one notices that the CIEA methodology can be applied to obtain relations between the the unknown derivatives ($\partial U/\partial Z|_{Z=X}$ and $\partial U/\partial Y|_{Z=X}$) and the averaged velocity $U_{av}(Y)$. Nevertheless, two different approximation alternatives arise:

1. Employ Hermite formulas for the integrals of $U(Y, Z)$ and $\partial U/\partial Z$.
2. Employ Hermite formulas for the integrals of $U(Y, Z)$ and $\partial U/\partial Y$.

Regardless of the chosen alternative, the usage of $H_{0,0}$ or $H_{1,1}$ formulas for $U(Y, Z)$, together with $H_{0,0}$ formulas for the derivatives of U, leads to approximation rules in the following form:

$$\left.\frac{\partial U}{\partial Z}\right|_{Z=X} = -\frac{1}{\xi} \left.\frac{\partial U}{\partial Y}\right|_{Z=X} \approx -\gamma_1 \frac{U_{av}}{\xi Y + \eta} + \frac{\gamma_2}{\xi} \frac{\mathrm{d}U_{av}}{\mathrm{d}Y}, \tag{11}$$

where γ_1 and γ_2 are constants whose values depend on the type of approximation used, and these will be determined in the next section. For rectangular ducts ($\eta = 1$ and $\xi = 0$), relation (10) does not hold, and only the first approximation alternative is possible. For these type of

ducts (with $\psi = \pi/2$), a general approximation relation without γ_2 is obtained:

$$\left.\frac{\partial U}{\partial Z}\right|_{Z=X} \approx -\gamma_1 U_{av}. \tag{12}$$

The solution of system (9) can be simplified according to the type of cross-section geometry. The most general case is the trapezoidal duct, whose solution is obtained from combining equation (11) with system (9), such that:

$$\frac{U_{av}(Y)}{G^*} = \zeta_1 (\xi Y + \eta)^{\gamma_3 + \chi} + \zeta_2 (\xi Y + \eta)^{\gamma_3 - \chi} + \zeta_3 (\xi Y + \eta)^2, \tag{13a}$$

with

$$\zeta_1 = -\frac{\zeta_3(1 - \eta^{-\gamma_3+\chi+2})}{1 - \eta^{2\chi}}, \tag{13b}$$

$$\zeta_2 = \frac{\zeta_3(\eta^{2\chi} - \eta^{-\gamma_3+\chi+2})}{1 - \eta^{2\chi}}. \tag{13c}$$

For triangular ducts, $K \to \infty$, and a simpler solution is obtained:

$$\frac{U_{av}(Y)}{G^*} = \zeta_6\Big((1 - Y)^2 - (1 - Y)^{\gamma_3 + \chi}\Big). \tag{14}$$

Similarly, for rectangular profiles, the combination of (12) and system (9) yields the following solution:

$$\frac{U_{av}(Y)}{G^*} = \frac{1}{K^2\gamma_1}\left(\frac{\cos h(K(Y - 1/2)\sqrt{\gamma_1})}{\cos h(K\gamma_1/2)} - 1\right). \tag{15}$$

The constants γ_3, χ, ζ_3, and ζ_6 are given by:

$$\gamma_3 = -\frac{1}{4}(1 + 2\gamma_2 + \cos(2\psi))\sec(\psi)^2, \tag{16a}$$

$$\chi = \sqrt{\gamma_1 (1 + \tan^2(\psi)) + \gamma_3^2}, \tag{16b}$$

$$\zeta_3 = \frac{\sin^2(\psi)}{K^2 (3 - \gamma_1 + 2\gamma_2 + 3\cos(2\psi))}, \tag{16c}$$

$$\zeta_6 = \frac{\cos^2(\psi)}{(3 - \gamma_1 + 2\gamma_2 + 3\cos(2\psi))}. \tag{16d}$$

Once the solution of the Z-averaged velocity field is obtained, the last step is the calculation of the friction factor itself. The value of Fanning friction factor can be obtained directly from using Eq. (6) and the calculated value of G^*, which is obtained from the definition of the cross-sectional averaged velocity in dimensionless form:

$$\frac{2}{1 + \eta}\int_0^1 (\xi Y + \eta) U_{av}(Y)\, dY = 1, \tag{17a}$$

such that the value of G^* can be calculated by substituting the expressions for the velocity U_{av} into the relation below:

$$G^* = \left(\frac{2}{1 + \eta}\int_0^1 (\xi Y + \eta)\frac{U_{av}}{G^*}\, dY\right)^{-1}. \tag{17b}$$

After substituting the averaged-velocity expressions into Eq. (17b), integrating the result and simplifying, closed-form expressions for calculating the friction factor are obtained. For rectangular ducts, $f\,\mathrm{Re}$ is given by

$$f\,\mathrm{Re} = \frac{8K^3\gamma_1^{3/2}}{(K + 2)^2\left(K\sqrt{\gamma_1} - 2\tanh\left(\frac{1}{2}K\sqrt{\gamma_1}\right)\right)}, \tag{18}$$

whereas for triangular ducts, the friction factor is given by:

$$f\,\mathrm{Re} = \frac{(\gamma_3 + \chi + 2)\sec^4(\psi/2)(\gamma_1 + 2(\gamma_3 - 1)\cos(2\psi) + 2\gamma_3 - 2)}{\gamma_3 + \chi - 2}. \tag{19}$$

For the trapezoidal duct, a more complicated expression is obtained, since it depends on two geometric parameters (K and ψ):

$$f\,\mathrm{Re} = -\frac{G^*(2K\cot(\psi) + 4)^2}{2(K(\cot(\psi) + \csc(\psi)) + 2)^2}, \tag{20a}$$

in which G^* is obtained from:

$$G^* = \left[-\frac{\zeta_1(2\eta(\gamma_3 + \chi + 2) - 2\eta^{\gamma_3+\chi}(\eta^2(\gamma_3 + \chi + 1) + ((\eta - 1)(\gamma_3 + \chi + 1) + \eta)\eta^{-\gamma_3-\chi}))}{(\eta^2 - 1)(\gamma_3 + \chi + 1)(\gamma_3 + \chi + 2)} + \right.$$
$$\left. -\frac{2\zeta_2\left(\eta - \eta^{\gamma_3-\chi+2} + \frac{\eta^{\gamma_3}\left(\eta^{2-\chi} - \eta^{-\gamma_3}((\eta-1)(\gamma_3-\chi+1)+\eta)\right)}{\gamma_3-\chi+2}\right)}{(\eta^2 - 1)(\gamma_3 - \chi + 1)} + \frac{1}{2}\zeta_3(\eta^2 + 1)\right]^{-1}. \tag{20b}$$

4 Coupled integral equations approach

Now that a general expression for the friction factor is available, the four different approximation schemes are carried-out, each leading to different values for the parameters γ_1 and γ_2. For the sake of simplicity, no Hermite approximations of order higher than $H_{1,1}$ are used and the $H_{1,1}$ approximation is used solely for the integral of $U(Y, Z)$.

4.1 Case 1: $H_{0,0}/H_{0,0}$ with alternative 1

In case 1, the $H_{0,0}$ approximation is used to yield expressions for the integrals of the velocity profile and its derivative with respect to Z:

$$\int_0^{X(Y)} U(Y,Z)\,\mathrm{d}Z \approx \frac{1}{2}\,(\xi\,Y+\eta)\,(U(Y,0)+U(Y,X(Y))), \tag{21a}$$

$$\int_0^{X(Y)} \frac{\partial U}{\partial Z}\,\mathrm{d}Z \approx \frac{1}{2}\,(\xi\,Y+\eta)\left(\left.\frac{\partial U}{\partial Z}\right|_{Z=0}+\left.\frac{\partial U}{\partial Z}\right|_{Z=X}\right). \tag{21b}$$

Once these equations are solved for the unknown potential and derivative, using the boundary information and the definition of the average potential, the following γ-values are obtained:

$$\gamma_1 = 4, \quad \gamma_2 = 0. \tag{21c}$$

4.2 Case 2: $H_{0,0}/H_{0,0}$ with alternative 2

For approximation case 2, the $H_{0,0}$ approximation is again used to yield expressions for the integral of the velocity profile (21a). However, instead of approximating the integral of the velocity's Z-derivative, the $H_{0,0}$ rule is used with the Y-derivative:

$$\int_0^{X(Y)} \frac{\partial U}{\partial Y}\,\mathrm{d}Z \approx \frac{1}{2}\,(\xi\,Y+\eta)\left(\left.\frac{\partial U}{\partial Y}\right|_{Z=0}+\left.\frac{\partial U}{\partial Y}\right|_{Z=X(Y)}\right). \tag{22a}$$

Solving the above equation, together with (21a), for the unknown potential and its derivative, and substituting the boundary information results in the following values for γ_1 and γ_2:

$$\gamma_1 = 2, \quad \gamma_2 = 0. \tag{22b}$$

4.3 Case 3: $H_{1,1}/H_{0,0}$ with alternative 1

For case 3, the $H_{0,0}$ approximation is used to yield an expression for the integral of the velocity's Z-derivative (21b), and, for the integral of the velocity profile, the $H_{1,1}$ approximation is used as follows:

$$\int_0^{X(Y)} U(Y,Z)\,\mathrm{d}Z \approx \frac{1}{2}\,(\xi\,Y+\eta)\,(U(Y,0)+U(Y,X)) + \\ + \frac{1}{12}\,(\xi\,Y+\eta)^2\left(\left.\frac{\partial U}{\partial Z}\right|_{Z=0}-\left.\frac{\partial U}{\partial Z}\right|_{Z=X}\right).$$

The above equation, together with (21b), is solved for the unknown potential and its derivative to give, and finally the following γ-values are obtained:

$$\gamma_1 = 3, \quad \gamma_2 = 0. \tag{23a}$$

4.4 Case 4: $H_{1,1}/H_{0,0}$ with alternative 2

For approximation case 4 ($H_{1,1}/H_{0,0}$ with alternative 2), the $H_{1,1}$ approximation is again used to yield expressions for the integral of the velocity profile, Eq. (23a). However, now the $H_{0,0}$ rule is applied to the integral of the Y-derivative [Eq. (22a)]. Solving Eqs. (21b) , (23a) and (22a) for the unknown potential and its derivative, yields after simplification:

$$\gamma_1 = 2, \quad \gamma_2 = -\frac{1}{2}. \tag{24}$$

5 Results and discussion

Now that the solution methodology has been presented, friction factor results for different cross-section geometries are presented. First, results are presented for comparing results among different approximation schemes, which will provide an indication of regions where each approximation scheme is better suited for application. Then, a combination of the proposed schemes based on simple weighted averaging is carried out for further improving the approximation error.

5.1 Rectangular ducts

For rectangular ducts, the following explicit expressions for the friction-factor are obtained:

$$f\,\mathrm{Re} = \frac{32\,K^3}{(K+2)^2\,(K-\tanh(K))}, \quad \text{for case 1,} \tag{25a}$$

$$f\,\mathrm{Re} = \frac{24\,K^3\,\sqrt{3}}{(K+2)^2\left(K\sqrt{3}-2\tanh\left(\frac{K}{2}\sqrt{3}\right)\right)}, \quad \text{for case 3.} \tag{25b}$$

The results of these approximations are then compared with two literature results. First, the exact analytical

solution to the problem, which is readily available for these types of ducts using the Classical Integral Transform Technique [22], is given by:

$$f\,\mathrm{Re} = \frac{24}{\left(\frac{1}{K}+1\right)^2}\left(1 - \frac{192}{\pi^5\,K}\sum_{n=1,3,\ldots}^{\infty}\frac{\tanh\left(\frac{n\pi K}{2}\right)}{n^5}\right)^{-1}, \qquad (26)$$

Then, an approximation for the solution, given by Shah and London [23]:

$$\frac{f\,\mathrm{Re}}{24} = 1 - 0.2537\,K^5 + 0.9564\,K^4 - 1.7012\,K^3 + 1.9467\,K^2 - 1.3553\,K. \qquad (27)$$

The results calculated for the two type of approximations are presented in Fig. 2, where the exact solution corresponds to Eq. (26) and that of reference [23] to Eq. (27), in which these two solutions overlap each other. As can be seen, case 3 ($H_{0,0}/H_{1,1}$) presents better results than case 1 ($H_{0,0}/H_{0,0}$), having a maximum relative error of almost 7%. It should also be noted that the error is not uniform, having an average value of about 6.1% for case 1 and 3.6% for case 3.

As an attempt to further improve the results, a combination of the $H_{0,0}/H_{1,1}$ and $H_{0,0}/H_{0,0}$ approximations is proposed. The combination is based on a weighted average in the following form:

$$(f\,\mathrm{Re})_{\mathrm{imp.}} = (f\,\mathrm{Re})_{\mathrm{case\,1}} + \frac{(f\,\mathrm{Re})_{\mathrm{case\,3}} - (f\,\mathrm{Re})_{\mathrm{case\,1}}}{K}, \qquad (28)$$

which yields the solution of case 1 for $K = 0$ and the solution of case 3 for $K = 1$. Although it may appear that this solution would lead to an infinite value of $f\,\mathrm{Re}$ for $K = 0$, this does not occur because at this position cases 1 and 3 yield the exact same result such that the second term in expression (28) is zero. The results of the proposed approximation are examined by plotting the relative errors in magnitude $|\epsilon|$, shown in Fig. 3.

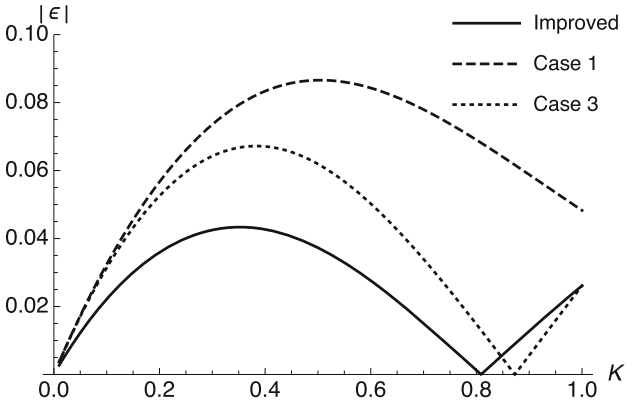

Fig. 3 Relative error in friction factor for rectangular duct for different approximation schemes

As can be seen from this figure, the error of the combined approximation scheme is just a little over four percent for the worst-case scenario, and it is always smaller than any of the other approximation cases, being clearly a better alternative.

5.1.1 Triangular ducts

For triangular ducts, a different expression for each approximation case is readily obtained for $f\,\mathrm{Re}$ in terms of the polygon angle ψ by substituting the γ-values in Eq. (19). The data are then compared with results presented by Shah and London [23], as displayed in Fig. 4. Naturally, the data for 0° and 90° are limiting cases in which the duct ceases to have an actual triangular form.

As one can observe, case 1 ($H_{0,0}/H_{0,0}$) cannot yield a good approximation for triangular ducts. On the other hand, case 3 ($H_{1,1}/H_{0,0}$) gives a satisfactory results for angles ranging from 55° to 90°, but looses accuracy for smaller angles. For triangular profiles with smaller angles ($\psi \leq 30°$) cases 2 ($H_{0,0}/H_{0,0}$) and 4 ($H_{1,1}/H_{0,0}$) provide a good approximation.

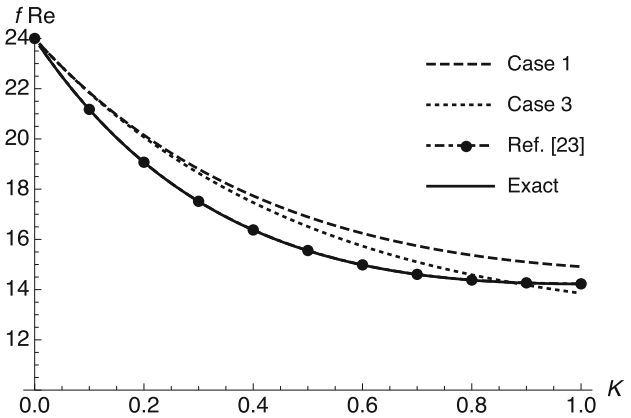

Fig. 2 Variation of friction factor in rectangular duct with aspect ratio

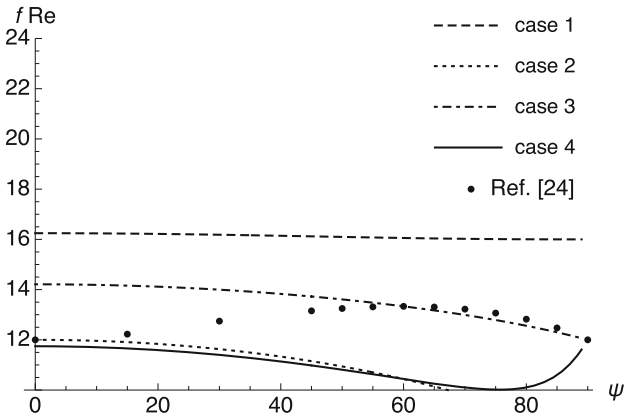

Fig. 4 Variation of friction factor in triangular duct with angle

From the presented results, it is clear that a weighted average between cases 3 and 4 can be proposed. Case 4 is chosen instead of case 2 for maintaining the same type of Hermite approximation. By combing these cases in a way in which cases 3 dominates for large angles and case 4 dominates for small angles a more uniform smaller error should be obtained. The proposed combination is written as:

$$(f\,\mathrm{Re})_{\mathrm{imp.}} = (f\,\mathrm{Re})_{\mathrm{case\,3}}\left(\frac{\psi}{\pi/2}\right) + (f\,\mathrm{Re})_{\mathrm{case\,4}}\left(1-\frac{\psi}{\pi/2}\right), \tag{29}$$

The relative error of this approximation is compared with that of the previous cases (only case 3 and 4), where the data from [23] was interpolated for calculating the error. The comparison can be seen on Fig. 5, which clearly shows a major improvement from using Eq. (29). With this approximation, the maximum error is below 3%, which is significantly smaller than that obtained for cases 3 and 4.

5.2 Trapezoidal ducts

The results for trapezoidal cross-section ducts are presented in Figs. 6 and 7, for various aspect ratios and trapezoid angles, using all four approximation alternatives. In order to analyze the trapezoidal profiled duct, exact solutions using the Generalized Integral Transform Technique (GITT) obtained from [24] were used for comparisons.

Figure 6 presents the variation of the friction factor with the trapezoid aspect ratio K for different angles. As can be seen, up to 75°, approximation cases 2 and 4 yield better results than the remaining cases, which shows the inadequacy of using the approximation alternative 2 for smaller angles. For larger angles, case 3 give reasonable results, which are in fact better than those for case 4. For instance, when $\psi = 85°$ case 4 moves away from the other curves, yielding the worst result, which shows that the combination

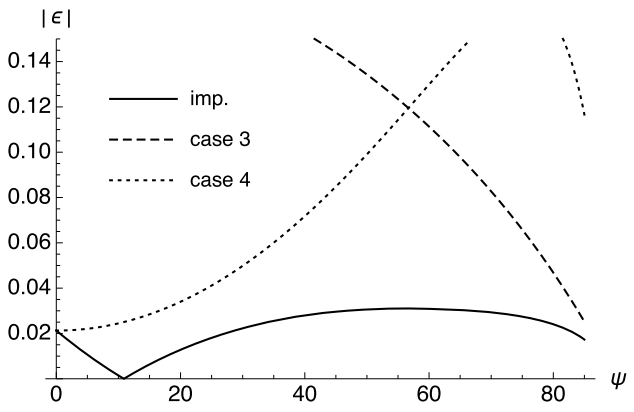

Fig. 5 Relative error in friction factor for triangular duct for different approximation schemes

of the $H_{1,1}/H_{0,0}$ approximation with approximation alternative 2 is not a good choice for large angles.

The next results, examine more closely the dependence of the friction factor on the trapezoid angle, by plotting $f\,\mathrm{Re}$ versus ψ for different aspect ratios, as presented in Fig. 7. These results demonstrate that for very small aspect ratios ($K = 0.01$), all approximation cases yield similar results – all of which are in very good agreement with the literature data. However, as K is increased up to 0.5, all approximations tend to generally overpredict the friction factor, with case 4 yielding the better results. Nevertheless for $K = 0.25$ case 4 already starts to exhibit an unsuited behavior for larger angles; this tendency is amplified as the aspect ratio is further increased. This seems suggests that approximation alternative 1 is better suited for smaller angles. This observation is confirmed when one notices that the cases with the $H_{0,0}/H_{0,0}$ approximation also give better results for smaller angles with the approximation alternative 1; for instance, case 2 is much better than case 1 for smaller angles.

With the previous observations in mind, as similarly done for the previous types of ducts, a combined approximation is proposed. The adopted strategy is similar to the one used for the triangle; however, due to the unsuitable behavior case 4 presents for large angles, case 2 and 3 are combined:

$$(f\,\mathrm{Re})_{\mathrm{imp.1}} = (f\,\mathrm{Re})_{\mathrm{case\,3}}\left(\frac{\psi}{\pi/2}\right) + (f\,\mathrm{Re})_{\mathrm{case\,2}}\left(1-\frac{\psi}{\pi/2}\right). \tag{30}$$

Although it is verified that first improvement provides a smaller error for larger aspect ratios, for smaller aspect ratios approximation case 2 is generally a better choice. Hence, a second improved formula is proposed, based again on a simple weighted average of the two limits:

$$(f\,\mathrm{Re})_{\mathrm{imp.2}} = (f\,\mathrm{Re})_{\mathrm{case\,2}}\,(1-K^2) + (f\,\mathrm{Re})_{\mathrm{imp.1}}\,K^2. \tag{31}$$

The results of using the improved expressions are presented in Fig. 8, which displays the relative error of the employed approximations compared with that of cases 2, 3 and 4.

The error of case 1 is generally larger than all these cases and therefore is not presented. As can be seen from this figure, the combined improved approximation schemes yield a much better homogeneous error behavior. Also, as previously anticipated, the results show that the first improved case, as given by Eq. (30), yields results that have a worse error when compared to approximation case 2. However, with the second improved approximation [Eq. (31)], is kept under 3% for most values of K and ψ. For smaller aspect rations (i.e. 0.25), the error becomes higher (about 5%), as all approximations cases move away from the exact solution.

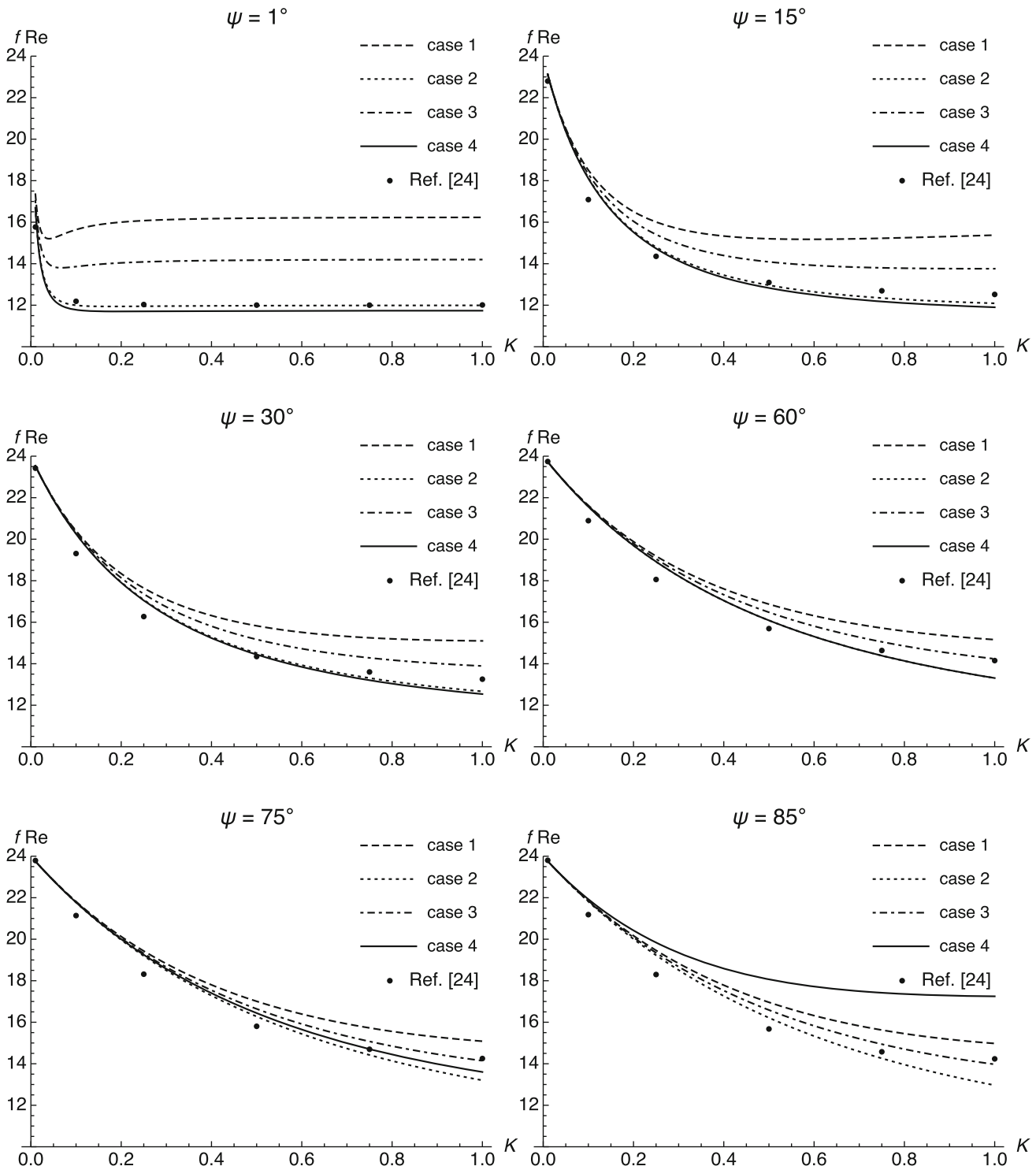

Fig. 6 Variation of friction factor in trapezoidal duct with aspect ratio for different angles

6 Conclusions

This paper presented an alternative approach for calculating friction-factor in steady laminar fluid flow in ducts of different polygonal cross-sections. An approximate analytical methodology, based on the coupled integral equations approach (CIEA) was utilized. Closed form analytical expressions were obtained for Fanning's friction factor, for various combination of polygon angles and aspect ratios. Results for four different approximation cases

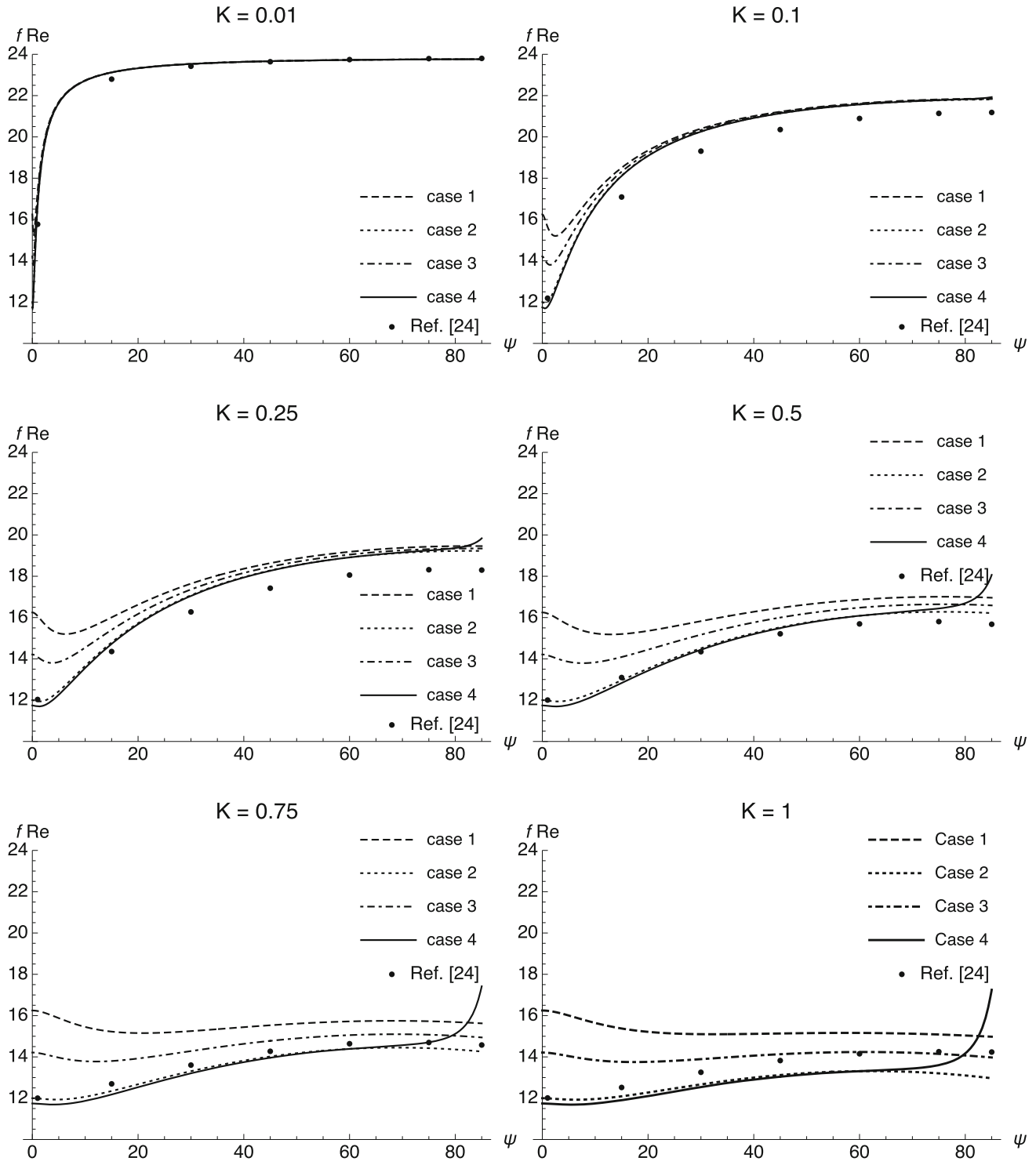

Fig. 7 Variation of friction factor in trapezoidal duct with angle for different aspect ratios

were presented, consisting of a combination of two levels of approximations and two approximation alternatives. The data was compared with previously published results, and an error analysis showed that some cases have better performance (smaller error) than others. In addition, the results showed that different approximation alternatives lead to larger errors for different values of the polygon angle. This non-uniform error distribution was corrected by employing a simple combination of approximation cases based on simple weighted averaging schemes, leading to

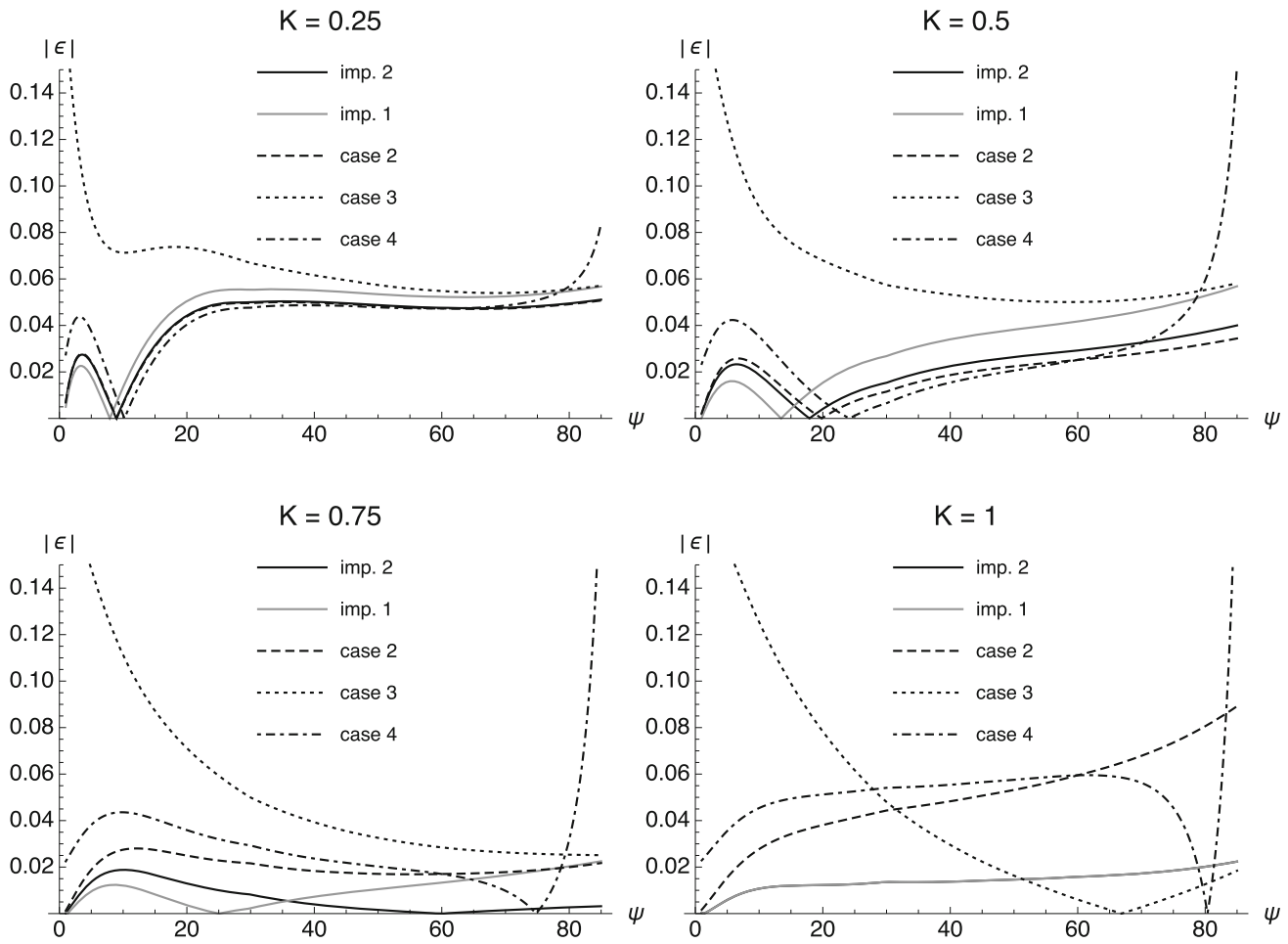

Fig. 8 Relative error in friction factor for trapezoidal duct for different approximation schemes

improved relations for calculating the friction-factor. The results of the improved schemes were able, in some cases, to maintain the maximum error under 3% in magnitude, which is generally acceptable for engineering applications.

Acknowledgements The authors would like to acknowledge the financial support provided by the Brazilizan Government funding agencies CAPES, CNPq, and FAPERJ.

References

1. Hermite M Ch. (1878) Sur la formule d'interpolation de Lagrange. J Crelle 84:70–79
2. Mennig J, Auerbach T, Hälg W (1983) Two point Hermite approximation for the solution of linear initial value and boundary value problems. Comput Methods Appl Mech Eng 39(2):199–224
3. Mennig J, Özişik MN (1985) Coupled integral equation approach for solving melting or solidification. Int J Heat Mass Transf 28(8):1481–1485
4. Aparecido JB, Cotta RM (1990) Improved one-dimensional fin solutions. Heat Transf Eng 11(1):49–59
5. Scofano-Neto F, Cotta RM (1992) Counterflow double-pipe heat exchanger analysis using a mixed lumped-differential formulation. Int J Heat Mass Transf 35:1723–1731
6. Scofano-Neto F, Cotta RM (1993) Improved hybrid lumped-differential formulation for double-pipe heat-exchanger analysis. J Heat Transf: ASME 115(4):921–927
7. Corrêa EJ, Cotta RM (1998) Enhanced lumped-differential formulations of diffusion problems. Appl Math Model 22(3):137–152
8. Reis MCL, Macêdo EN, Quaresma JNN (2000) Improved lumped-differential formulations in hyperbolic heat conduction. Int Commun Heat Mass Transf 27(7):965–974
9. Jian Su (2004) Improved lumped models for transient radiative cooling of a spherical body. Int Commun Heat Mass Transf 31(1):85–94
10. Ruperti NJ, Cotta RM, Falkenberg CV, Su J (2004) Engineering analysis of ablative thermal protection for atmospheric reentry: improved lumped formulations and symbolic-numerical computation. Heat Transf Eng 25(6):101–111
11. Dantas LB, Orlande HRB, Cotta RM (2007) Improved lumped-differential formulations and hybrid solution methods for drying in porous media. Int J Therm Sci 46(9):878–889
12. Ge Su, Tan Zheng, Jian Su (2009) Improved lumped for transient heat conduction in a slab with temperature-dependent thermal conductivity. Appl Math Model 33(1):274–283

13. Tan Z, Su G, Su J (2009) Improved lumped models for combined convective and radiative cooling of a wall. Appl Therm Eng 29(11–12):2439–2443
14. An C, Su J (2011) Improved lumped models for transient combined convective and radiative cooling of multi-layer composite slabs. Appl Therm Eng 31(14–15):2508–2517
15. Keshavarz P, Taheri M (2007) An improved lumped analysis for transient heat conduction by using the polynomial approximation method. Heat Mass Transf 43(11):1151–1156
16. Sadat H (2005) A general lumped model for transient heat conduction in one-dimensional geometries. Appl Therm Eng 25(4):567–576
17. Sadat H (2006) A second order model for transient heat conduction in a slab with convective boundary conditions. Appl Therm Eng 26(8):962–965
18. Sphaier LA, Jurumenha DS (2012) Improved lumped-capacitance model for heat and mass transfer in adsorbed gas discharge operations. Energy 44(1):985
19. An Chen, Jian Su (2013) Lumped parameter model for one-dimensional melting in a slab with volumetric heat generation. Appl Therm Eng 60(1–2):387–396
20. Underwood CP (2014) An improved lumped parameter method for building thermal modelling. Energy Build 79:191–201
21. An Chen, Jian Su (2015) Lumped models for transient thermal analysis of multilayered composite pipeline with active heating. Appl Therm Eng 87:749–759
22. Mikhailov MD, Özişik MN (1984) Unified analysis and solutions of heat and mass diffusion. Wiley, New York
23. Shah RK, London AL (1978) Laminar flow forced convection in ducts: a source book for compact heat exchanger analytical data. In: Irvine TF Jr, Hartnet JP (eds) Advances in heat transfer. Academic Press, New York
24. Aparecido JB (1988) Transformada Integral Generalizada no Escoamento Laminar e Transferência de Calor em Dutos Retilíneos de Geometria Arbitrária